Fluids and Barriers of the CNS

RESEARCH

Open Access

Relaxation-exchange magnetic resonance imaging (REXI): a non-invasive imaging method for evaluating trans-barrier water exchange in the choroid plexus

Xuetao Wu[1,2†], Qingping He[3,4†], Yu Yin[5], Shuyuan Tan[6], Baogui Zhang[1,2], Weiyun Li[7], Yi-Cheng Hsu[8], Rong Xue[1,2*] and Ruiliang Bai[4,7*]

Abstract

Background The choroid plexus (CP) plays a crucial role in cerebrospinal fluid (CSF) production and brain homeostasis. However, non-invasive imaging techniques to assess its function remain limited. This study was conducted to develop a novel, contrast-agent-free MRI technique, termed relaxation-exchange magnetic resonance imaging (REXI), for evaluating CP-CSF water transport, a potential biomarker of CP function.

Methods REXI utilizes the inherent and large difference in magnetic resonance transverse relaxation times (T_2s) between CP tissue (e.g., blood vessels and epithelial cells) and CSF. It uses a filter block to remove most CP tissue magnetization (shorter T_2), a mixing block for CP-CSF water exchange with mixing time t_m, and a detection block with multi-echo acquisition to determine the CP/CSF component fraction after exchange. The REXI pulse sequence was implemented on a 9.4 T preclinical MRI scanner. For validation of REXI's ability to measure exchange, we conducted preliminary tests on urea-water proton-exchange phantoms with various pH levels. We measured the steady-state water efflux rate from CP to CSF in rats and tested the sensitivity of REXI in detecting CP dysfunction induced by the carbonic anhydrase inhibitor acetazolamide.

Results REXI pulse sequence successfully captured changes in the proton exchange rate (from short-T_2 component to long-T_2 component [i.e., k_{sl}]) of urea-water phantoms at varying pH, demonstrating its sensitivity to exchange processes. In rat CP, REXI significantly suppressed the CP tissue signal, reducing the short-T_2 fraction (f_{short}) from 0.44 to 0.23 ($p<0.0001$), with significant recovery to 0.28 after a mixing time of 400 ms ($p=0.014$). The changes in f_{short} at various mixing times can be accurately described by a two-site exchange model, yielding a steady-state water efflux rate from CP to CSF (i.e., k_{bc}) of 0.49 s^{-1}. A scan-rescan experiment demonstrated that REXI had excellent reproducibility in measuring k_{bc} (intraclass correlation coefficient = 0.90). Notably, acetazolamide-induced CSF reduction resulted in a 66% decrease in k_{bc} within rat CP.

†Xuetao Wu and Qingping He contributed equally to this manuscript.

*Correspondence:
Rong Xue
rxue@ibp.ac.cn
Ruiliang Bai
ruiliangbai@zju.edu.cn
Full list of author information is available at the end of the article

Conclusions This proof-of-concept study demonstrates the feasibility of REXI for measuring trans-barrier water exchange in the CP, offering a promising biomarker for future assessments of CP function.

Keywords Choroid plexus, Blood cerebrospinal fluid barrier, Contrast-agent-free, Relaxation exchange, Magnetic resonance imaging

Background

Located within the ventricles, the choroid plexus (CP) is responsible for cerebrospinal fluid (CSF) secretion and forms the blood-cerebrospinal fluid barrier (BCSFB). It comprises a highly vascularized stroma (including connective tissue, pericytes, and fenestrated blood vessels distinct from those of the blood–brain barrier), covered by a single layer of epithelial cells [1]. The CP serves as a vital exchange interface between blood and CSF, where nutrients are imported and metabolites are exported, supporting brain homeostasis [2, 3]. CSF, secreted in the lateral ventricles, circulates through the foramen of Monro to the third ventricle, then proceeds through the aqueduct of Sylvius to the fourth ventricle. From there, it can either enter the spinal cord or be reabsorbed into the lymphatic system within the subarachnoid space [4].

The CP is a crucial component of CSF circulation. Inadequate CSF production can significantly hinder brain development [4], Conversely, excessive CSF (due to hypersecretion, obstructed flow, or limited reabsorption) can lead to hydrocephalus and idiopathic intracranial hypertension [4, 5]. BCSFB dysfunction is also associated with a wide range of pathophysiological conditions, including neurodegenerative disorders such as Alzheimer's disease [6–8]. Although there is increasing research interest in the connections among circadian rhythm, sleep, the orexinergic system, and neurodegenerative diseases, the role of the CP in this context has not been fully elucidated [9, 10].

Thus far, the lack of non-invasive imaging techniques to quantify CP function has hindered a robust understanding of the BCSFB. Currently, net CSF secretion is often assessed using the indirect tracer dilution method, an invasive approach primarily applicable to experimental animals [11]. Furthermore, this method's estimate of CSF secretion includes contributions from CP tissue and potential extrachoroidal sources (e.g., blood–brain barrier and CSF-parenchyma interface) [12], making it difficult to fully determine the involvement of the BCSFB. Another direct method for measuring CSF secretion involves collecting CSF from the subarachnoid space, either in the cisterna magna or via lumbar puncture [13–15]. This approach is also invasive, interfering with intracranial pressure and potentially leading to incomplete collection [12]. Recently, the water efflux rate from the CP to CSF was suggested to constitute a sensitive biomarker of BCSFB integrity [16]; significant decreases have been observed in aged mice [16] and patients with mild cognitive dysfunction [17]. Specific magnetic resonance imaging (MRI) methods have been developed to measure this water efflux rate, either using contrast agents [17] or by adapting arterial spin labeling (ASL) without contrast agents [16, 18]. However, the options for MRI techniques in this area remain limited.

In this study, we propose a novel, contrast-agent-free MRI method and mechanism, termed relaxation-exchange magnetic resonance imaging (REXI), to measure the steady-state water efflux rate from CP to CSF (i.e., "k_{bc}"). REXI utilizes the large difference in transverse relaxation time (T_2) between blood and CSF (e.g., measured $T_2 = 30$ ms [19] and 300 ms [20] for arterial blood and CSF on 9.4 T MRI, respectively). It applies a specific MRI sequence and analysis method to measurement of the k_{bc}. Furthermore, REXI uses a filter block with an optimized echo time (TE_f) to first filter out CP water magnetization, then stores the magnetization back in the longitudinal direction, varies the mixing time (t_m) for water exchange between blood and CSF, and finally implements a detection block with multi-echo (ME) acquisition to quantify the water transported from CP to CSF and vice versa (Fig. 1A).

We validated the feasibility of REXI for measuring exchange in urea-water phantoms, where the pH was adjusted to vary proton exchange between urea and water. This phantom was chosen because it is a well-established two-site exchange system with distinct T_2s for each proton site [21–24] (urea protons have a shorter T_2 than water protons, e.g., the T_2 values of urea and water proton are ~ 40 and ~ 200 ms at 7 T, respectively [23]). Importantly, the proton exchange rates can be manipulated by altering pH [25], allowing validation of REXI sensitivity for exchange process detection. To ensure reproducibility, we conducted a scan-rescan experiment in rats. Additionally, we demonstrated the specificity of REXI in detecting CP function by intravenous injection of acetazolamide, a carbonic anhydrase inhibitor that significantly reduces CSF secretion [26, 27].

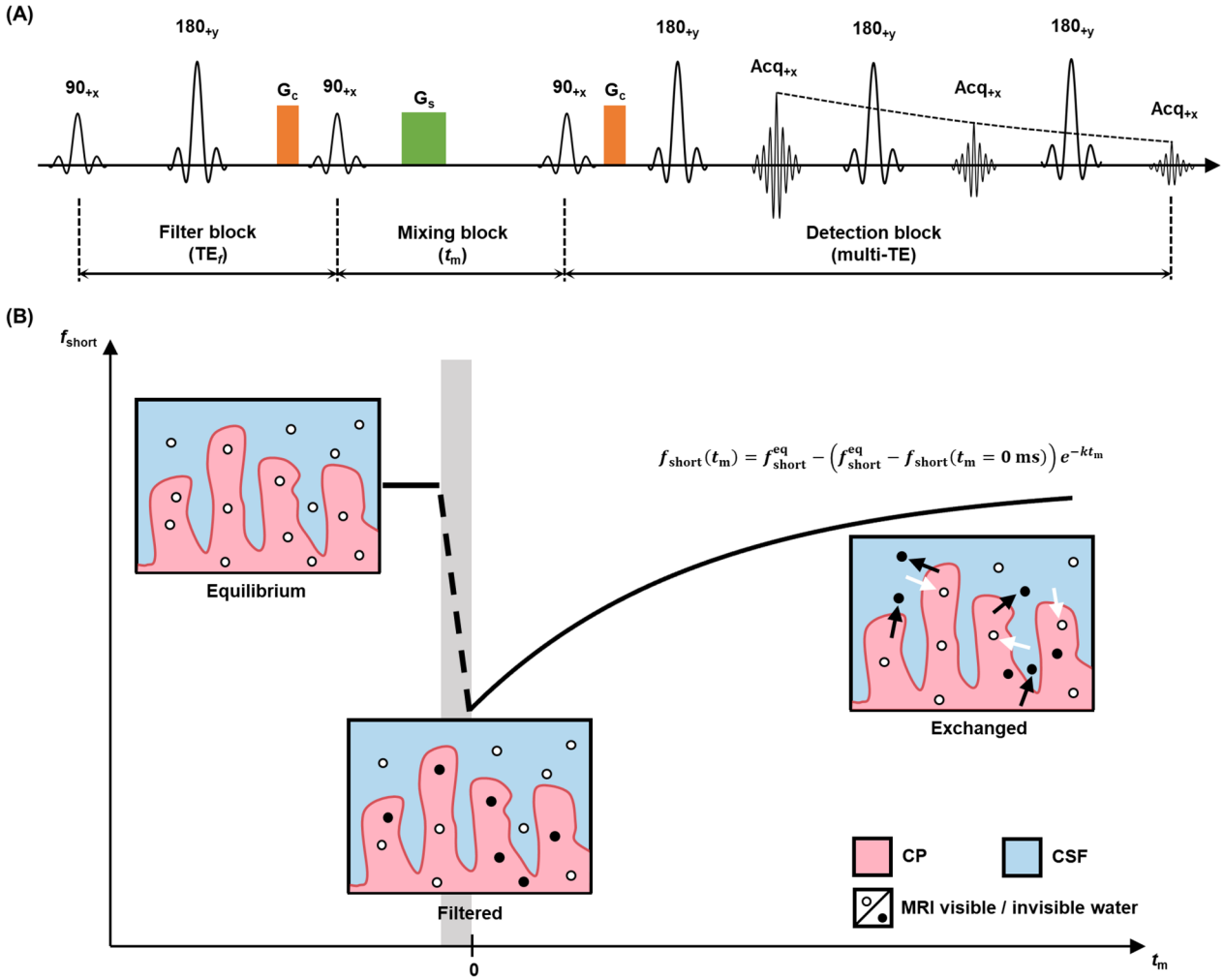

Fig. 1 Principles of REXI in the measurement of CP function. **A** Pulse sequence diagram of REXI, comprising a filter block with fixed echo time (TE_f), a mixing block with varying mixing time (t_m), and a detection block with multi-echo acquisition (TE). Paired crusher gradients (G_c) for coherence pathway selection are added before the second 90° pulse and after the third 90° pulse. A spoiler gradient (G_s) is applied to eliminate unwanted transverse magnetization in the mixing block. Pulses in the filter and detection blocks are non-selective and selective, respectively. **B** Illustration of REXI in the measurement of water transport from CP to CSF. When the filter is applied (gray shade), water molecules in blood become largely undetectable by MRI (filled dots), whereas those in CSF remain largely unfiltered, leading to a reduction in the short-T_2 component (i.e., CP) from f_{short}^{eq} to $f_{short}(t_m = 0\ ms)$ (dashed line). After a specific mixing time, water exchange between blood and CSF results in the recovery of f_{short} from $f_{short}(t_m = 0\ ms)$ to f_{short}^{eq}, and the recovery rate can be described by the water exchange rate k and Eq. (1)

Methods

REXI sequence and theory

REXI was designed to comprise a filter block with echo time TE_f, a mixing block with mixing time (t_m), and a detection block with multi-echo acquisition (multi-TE) (Fig. 1A). In the filter block, a spin echo with a T_2-weighting factor TE_f was applied to largely suppress the magnetization of short-T_2 components (e.g., CP tissue) while minimizing the impact on long-T_2 components (e.g., CSF) (Fig. 1B). In the subsequent mixing block, all rewound magnetization after the filter block was stored back in the longitudinal direction and maintained for a mixing time t_m. A spoiler gradient was inserted during this mixing time to dephase any transverse magnetization excited by the second 90° pulse. After a specific mixing time, the magnetization was excited back to the transverse plane, and a multiple spin echo sequence was applied to detect the magnetization fractions of various T_2 components. A pair of identical gradients was implemented before the second 90° pulse and after the third 90° pulse, forming a stimulated echo after the second gradient. In REXI, TE_f and

TEs in the filter and detection blocks were fixed; only t_m was varied to shorten the total scan time.

For a two-site system with distinguishable T_2s, such as the CP-CSF system, the magnetization fraction of the short-T_2 component measured in the detection block at a specific t_m, denoted $f_{short}(t_m)$, can be described as [28–31]:

$$f_{short}(t_m) = f_{short}^{eq} - \left(f_{short}^{eq} - f_{short}(t_m = 0ms)\right)e^{-kt_m} \quad (1)$$

where f_{short}^{eq} is the magnetization fraction of the short-T_2 component at equilibrium, $f_{short}(t_m = 0$ ms) is the f_{short} immediately after the filter block (determined by the T_2s of the two components and the TE_f used), and k is the exchange rate constant of the system. Here, we assume that the T_1s of the two components are identical. For an equilibrium or steady-state system:

$$f_{short}^{eq} k_{sl} = (1 - f_{short}^{eq}) k_{ls} \quad (2)$$

where k_{sl} is the steady-state water exchange rate from the short-T_2 component to the long-T_2 component, and k_{ls} describes the reverse flux rate. The relation between k and k_{sl} is as follows:

$$k = k_{sl} + k_{ls} = k_{sl}/(1 - f_{short}^{eq}) \quad (3)$$

REXI measures the water exchange rate between the two components by varying t_m and fitting **Eq.** (1).

Urea-water phantom for REXI validation

In the urea-water system, a well-established two-pool exchange system in the nuclear magnetic resonance (NMR) spectroscopy field [21–24], exchange occurs between the amide protons of urea (short-T_2 component) and the protons in water (long-T_2 component). Twelve urea-water phantoms at two different pH values (6.7 and 7.0, n = 6 at each pH) with fixed urea-water proton ratio of 30%/70% were used. The stock solution of urea-water phantoms was prepared by dissolving 36.5 g of urea powder in 50 mL of phosphate-buffered saline (pH = 7.4), then adding 0.05 mM $MnCl_2$ to reduce T_2. The pH of the urea solution was titrated with HCl, and the solution was transferred into 5-mm NMR tubes. The urea-water phantom experiment was completed within 4 h of solution preparation to ensure phantom stability.

Animal preparation

All animal experiments were approved by the Animal Experimentation Committee of Zhejiang University. Eight male Wistar Kyoto (WKY) rats aged 11–12 weeks were used in the scan-rescan reproducibility experiment. To verify the specificity of REXI in measuring the steady-state water efflux rate from CP to CSF, we administered either acetazolamide solution (n = 7, 20 mg ml^{-1}, 5 ml kg^{-1} body weight) or a vehicle control (n = 7, equiosmolar 1.4% NaCl solution, 5 ml kg^{-1} body weight) via intravenous (i.v.) tail vein injection to male WKY rats aged 3–4 months. Acetazolamide solution and vehicle preparation and administration were conducted as previously described [27]. All rats were anesthetized using 3% isoflurane, with a maintenance dose of approximately 2.5% isoflurane throughout the MRI scan.

MRI scanning protocols

All MRI scans were performed on a 9.4 T preclinical MRI scanner (BioSpec 94/30, Bruker, Ettlingen, Germany). Urea-water phantom experiments were conducted with a birdcage volume coil provided by the scanner vendor; rat experiments were carried out with a four-channel surface coil provided by the vendor.

Equilibrium multiple echo data were acquired using the Bruker-provided Multi-slice Multi-echo (MSME) sequence. For the urea-water phantom, MSME parameters were: repetition time (TR) = 2500 ms, echo time (TE) = 7 ms, number of echoes (NE) = 30, number of averages (NA) = 1, matrix = 64 × 64, field of view (FOV) = 28 mm × 28 mm, single slice with thickness = 2.0 mm, and scan time = 2 min 40 s. Single-slice REXI acquisition was conducted with the same spatial settings as MSME sequence and performed at four mixing times (t_m = 25, 100, 200, and 400 ms), with TR = 2500 ms + t_m, TE_f = 30 ms, and approximate total scan time for the four REXI acquisitions = 11 min 30 s. The REXI detection block was identical to that of the MSME sequence.

For the in vivo rat experiments, MRI scans included two-dimensional Rapid Acquisition with Relaxation Enhancement (RARE) T_2-weighted (T_2w) images, MSME, and REXI. T_2w anatomical images were acquired with the following parameters: TR = 2200 ms, TE = 8.5 ms, RARE factor = 8, NA = 3, matrix = 256 × 256, FOV = 35 mm × 35 mm, slice thickness = 0.5 mm, and approximate scan time = 3 min 31 s. Based on the T_2w anatomical images, a 1.5-mm-thick axial slice was carefully positioned to center on the caudal aspect of the lateral ventricles for MSME and REXI scans. A single-slice MSME sequence was performed with the following parameters: TR = 2500 ms, TE = 7 ms, NE = 30, NA = 1, matrix = 128 × 96, FOV = 35 mm × 35 mm, and scan time = 4 min. Single-slice REXI acquisition was repeated with four mixing times (t_m = 25, 100, 200, and 400 ms). For the REXI scan, the unique parameters were TR = 2500 ms + t_m, TE_f = 30 ms, and approximate total scan time for the four REXI acquisitions = 17 min 10 s; the remaining acquisition parameters were identical to those of the MSME scan. The varying TR is used to ensure the longitudinal magnetization has the same recovery time after the third 90°

pulse, which works as a saturation pulse leaving all longitudinal magnetization into the transverse plane. In the scan-rescan reproducibility experiment, the MSME and REXI scans were repeated within the same session. For the acetazolamide experiment, acetazolamide solution or vehicle was administered 40 min before the MSME and REXI scans. This timing was chosen to ensure that acetazolamide reached and maintained a steady uptake level during MSME and REXI acquisition, in accordance with a previous study [27].

MRI data postprocessing and k_{sl}/k_{bc} quantification

The MSME data were treated as the equilibrium state. The equilibrium magnetization fraction and T_2 values of the two components were obtained by fitting the MSME data S(TE) with a bi-exponential function:

$$S(\mathrm{TE}) = S_0\left(f_{\mathrm{short}}^{\mathrm{eq}} e^{-\mathrm{TE}/T_{2,\mathrm{short}}} + (1 - f_{\mathrm{short}}^{\mathrm{eq}}) e^{-\mathrm{TE}/T_{2,\mathrm{long}}}\right) \quad (4)$$

where $T_{2,\,\mathrm{short}}$ and $T_{2,\,\mathrm{long}}$ are the T_2 values of the short-T_2 and long-T_2 components, respectively. To obtain $f_{\mathrm{short}}(t_m)$ at each t_m in REXI, the ME data acquired in the REXI detection block were also fitted to Eq. (4); however, $T_{2,\,\mathrm{short}}$ and $T_{2,\,\mathrm{long}}$ were fixed to the values obtained from MSME data. Then, the water exchange rate constant k was obtained by fitting the resulting $f_{\mathrm{short}}(t_m)$ values to Eq. (1), with $f_{\mathrm{short}}(t_m = 0\ \mathrm{ms})$ and k as the only free parameters in the non-linear fitting equation. Finally, the exchange rate from the short-T_2 component to the long-T_2 component k_{sl} (i.e., the steady-state water efflux rate from CP to CSF, k_{bc}, in the rat CP) was estimated using Eq. (3). All non-linear fitting steps were performed using the lsqnonlin function in MATLAB (R2023b, The MathWorks Inc., Natick, MA, USA) with bound constraints of $0 \le T_{2,\,\mathrm{short}} \le 100$ ms, $0 \le T_{2,\,\mathrm{long}} \le 500$ ms, $0 \le f_{\mathrm{short}} \le 1$, and $0 \le k_{sl} \le 10\ \mathrm{s}^{-1}$.

In the urea-water phantom studies, the region of interest (ROI) was the entire cross-section of each phantom. In the rat experiments, ROIs within the bilateral CP were carefully drawn on high-resolution T_2w images and downsampled to REXI images using the imresize function in MATLAB. All ROIs were segmented with ITK-SNAP software, and all postprocessing was performed in MATLAB.

Statistical analysis

Mann–Whitney tests were performed to assess differences in k_{sl} between the two groups of urea-water phantoms at varying pH levels. For the scan-rescan reproducibility experiment, results were analyzed using Bland–Altman (BA) plots, intraclass correlation coefficients (ICCs), and coefficients of variation (CVs). We also utilized the Akaike Information Criterion (AIC) model [32] to evaluate the goodness of fit for mono-exponential and bi-exponential models. A smaller AIC value indicated a better fitting model. The Friedman test was used for comparisons of $f_{\mathrm{short}}^{\mathrm{eq}}$, $f_{\mathrm{short}}(t_m = 25\ \mathrm{ms})$ and $f_{\mathrm{short}}(t_m = 400\ \mathrm{ms})$ to validate the filter and mixing block functions in REXI. For the acetazolamide experiment in rats, Mann–Whitney tests were performed to compare k_{bc} in the CP between the treatment (i.v. delivery of acetazolamide) and control (i.v. delivery of vehicle) groups. Statistical analyses were performed using MATLAB and GraphPad Prism 9.

Results

Urea-water phantom experiments validated REXI's ability to measure exchange

For validation of REXI's ability to measure proton exchange, we conducted preliminary tests on urea-water phantoms with various pH levels, which altered the proton exchange rate between water and urea. The raw MSME and REXI images showed no apparent artifacts (Fig. 2A). As expected, REXI signals decreased with increasing mixing times due to T_1 effects, and all were lower than the MSME signals due to the filter block (Fig. 2B). Figure 2C displays the $f_{\mathrm{short}}(t_m)$ values calculated using Eq. (4) at four different mixing times. The $f_{\mathrm{short}}(t_m)$ values gradually recovered with increasing t_m and demonstrated good fit with Eq. (1). The 2SXM accurately fit the f_{short}-t_m curves, yielding exchange rates of $k_{sl} = 3.16 \pm 0.32\ \mathrm{s}^{-1}$ at pH = 6.7 and $1.98 \pm 0.39\ \mathrm{s}^{-1}$ at pH = 7.0 ($p = 0.0022$, Fig. 2D). Additionally, both $T_{2,\,\mathrm{short}}$ (16.45 ± 0.23) and $T_{2,\,\mathrm{long}}$ (66.84 ± 0.15) values at pH = 6.7 were significantly shorter than $T_{2,\,\mathrm{short}}$ (17.00 ± 0.40) and $T_{2,\,\mathrm{long}}$ (72.84 ± 0.36) values at pH = 7.0 ($p = 0.0152$ and 0.0022, respectively). There were no significant differences in $f_{\mathrm{short}}^{\mathrm{eq}}$ values (both 0.304 ± 0.002, $p > 0.9999$) between the two groups of urea-water phantoms at different pH levels.

REXI can capture water exchange between CP and CSF in rats

Representative MSME and REXI images as a function of t_ms are shown in Fig. 3A. We carefully delineated ROIs of the CP on high-resolution T_2w images as shown in Fig. 3B because the CP exhibits a shorter T_2 with lower T_2w signals relative to CSF in the lateral ventricles. Signals within the CP ROI of the MSME images and REXI images at each t_m were averaged and fitted using the bi-exponential Eq. (4) and mono-exponential $S(\mathrm{TE}) = S_0 e^{-\mathrm{TE}/T_2}$, respectively (Fig. 3C). Bi-exponential fitting was clearly superior, with substantially lower AIC values (-297.64 ± 19.26, n = 16 from scan-rescan experiments) relative to mono-exponential fitting (-219.12 ± 13.87). These results confirmed that

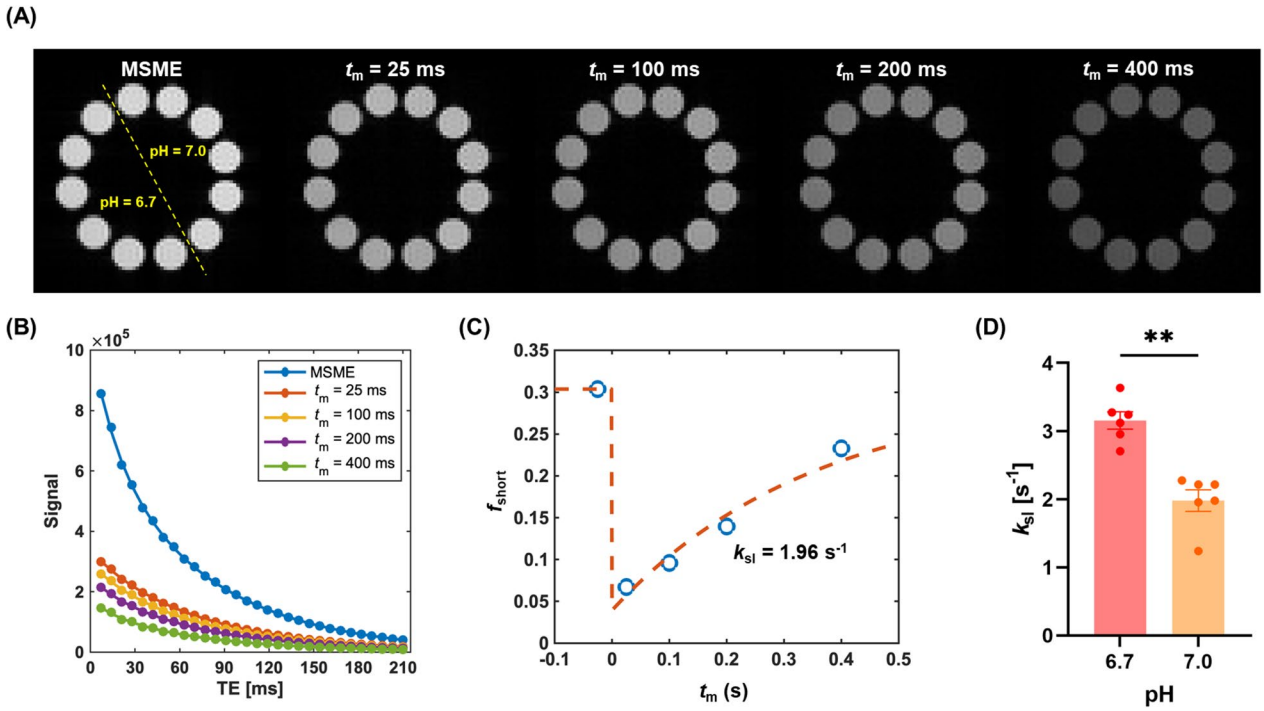

Fig. 2 Raw images and fitting results of REXI in measuring proton exchange within urea-water phantoms. **A** MSME and REXI images with minimum TE = 7 ms. **B** Signal decays of MSME and REXI at different t_ms and **C** the f_{short}-t_m curve from one representative phantom at pH = 7.0. In (**B**), filled blue circles represent MSME and REXI data, and curves are the results of model fitting to Eq. (4). In (**C**), the first circle at $t_m < 0$ denotes the f_{short}^{eq} estimated from MSME data; other circles represent the $f_{short}(t_m)$ values estimated from REXI data, and dashed curves are the results of model fitting to Eq. (1). **D** Statistical comparison of k_{sl} between the two groups at different pH values using Mann–Whitney tests. Data points (black dots) are overlaid on the corresponding box plots. Bar height and error bar width represent the mean and standard error of the mean (s.e.m.), respectively (same for subsequent figures). ** $p < 0.01$, * $p \leq 0.05$

bi-exponential fitting was more appropriate for the MSME and REXI signals. As shown in Fig. 3D, REXI significantly suppressed the CP signal and reduced the short-T_2 fraction f_{short} from $f_{short}^{eq} = 0.44 \pm 0.08$ to $f_{short}(t_m = 25\ ms) = 0.23 \pm 0.05$ (Friedman test, n = 16 from scan-rescan experiments, $p < 0.0001$), demonstrating the effectiveness of the REXI filter block. Subsequently, f_{short} values recovered to $f_{short}(t_m = 400\ ms) = 0.28 \pm 0.05$ ($p = 0.014$) due to water exchange between the CP and CSF during the mixing block. Notably, $f_{short}(t_m = 400\ ms)$ remained significantly lower than f_{short}^{eq} ($p = 0.014$), implying a relatively slow exchange. The representative f_{short}-t_m curve in Fig. 3E demonstrates that the 2SXM accurately fit the REXI data.

REXI demonstrated high reproducibility in measuring the steady-state water efflux rate from the CP to CSF in rats

To further validate the reproducibility of REXI, we measured the steady-state water efflux rate from CP to CSF (k_{bc}) in rats (n = 8). In the initial scan experiment, $k_{bc} = 0.46 \pm 0.37\ s^{-1}$, $f_{short}^{eq} = 0.45 \pm 0.09$, $T_{2,\ short} = 36.78 \pm 2.14$ ms, and $T_{2,\ long} = 257.03 \pm 43.77$ ms. In the rescan experiment, $k_{bc} = 0.52 \pm 0.47\ s^{-1}$, $f_{short}^{eq} = 0.44 \pm 0.08$, $T_{2,\ short} = 38.64 \pm 3.42$ ms, and $T_{2,\ long} = 253.90 \pm 35.28$ ms. As shown in Fig. 4, we analyzed these parameters using BA plots, ICCs, and CVs. Among the four parameters, k_{bc} showed a relatively high ICC of 0.90, despite exhibiting the highest CV (40%).

REXI can capture acetazolamide-induced CP dysfunction

Finally, we tested the sensitivity of REXI in detecting CP dysfunction induced by the carbonic anhydrase inhibitor acetazolamide. The treatment group (n = 7) underwent i.v. delivery of acetazolamide, whereas the control group (n = 7) underwent i.v. delivery of vehicle. The f_{short}-t_m curves of representative animals from each group are presented in Fig. 5A. Acetazolamide administration led to a 66% reduction in the CP steady-state water efflux rate ($k_{bc} = 0.22 \pm 0.11\ s^{-1}$) compared with the vehicle control ($k_{bc} = 0.66 \pm 0.33\ s^{-1}$, $p = 0.0012$). Conversely, the remaining three parameters showed no significant differences between the two groups (Fig. 5B): $f_{short}^{eq} = 0.36 \pm 0.04$ (treatment) vs. 0.34 ± 0.07 (control, $p = 0.2593$); $T_{2,\ short} = 43.71 \pm 3.03$ ms (treatment) vs. 41.01 ± 2.48 ms (control, $p = 0.1649$); and $T_{2,\ long} = 268.75 \pm 14.61$ ms (treatment) vs. 285.43 ± 16.49

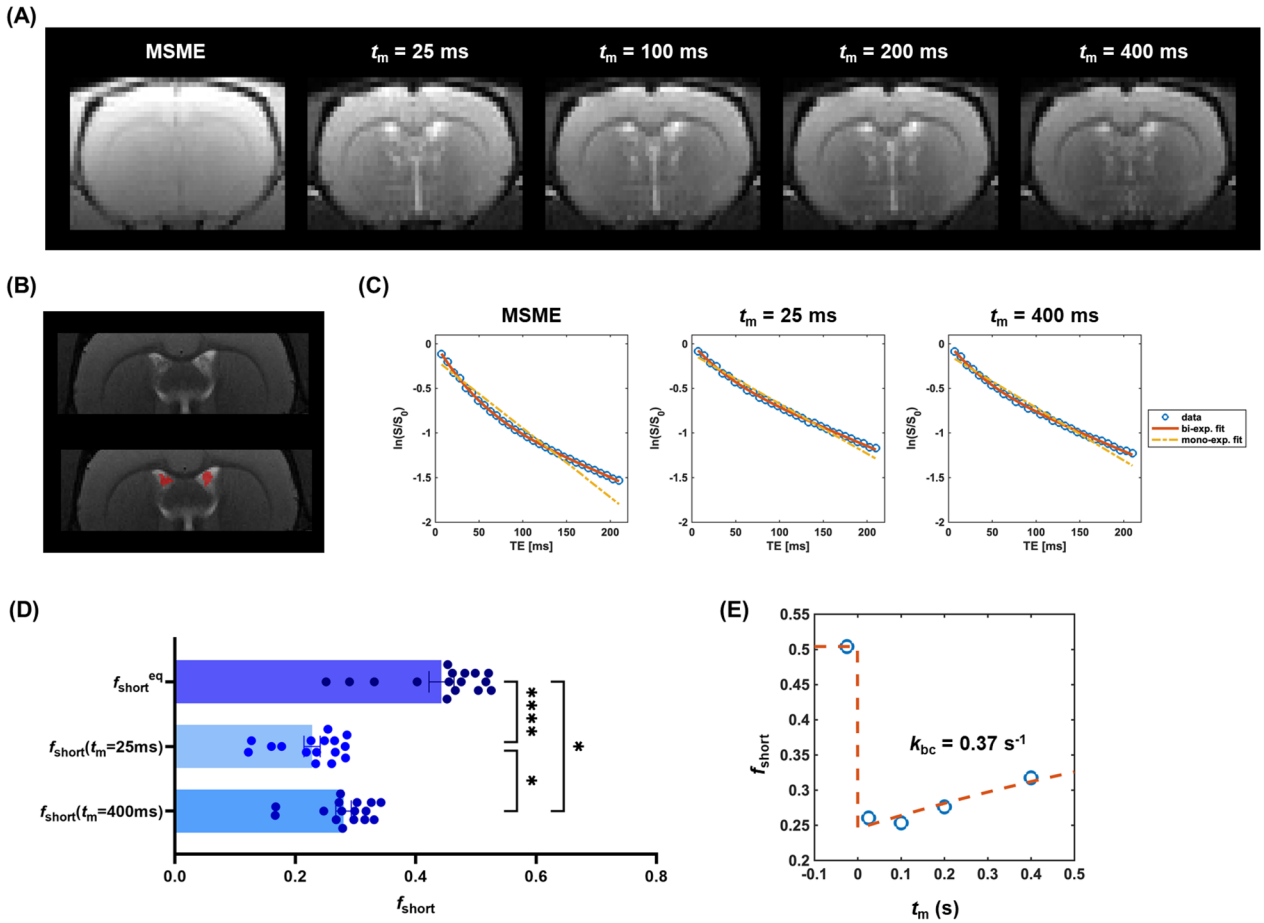

Fig. 3 Raw images and fitting results of REXI in measuring water exchange within the rat CP. **A** MSME and REXI images with minimum TE = 7 ms at each t_m, **B** T_2w anatomical image and corresponding ROI of the CP, and **C** signal decays of MSME and REXI at different t_ms from a representative rat. **D** Statistical comparison between f_{short}^{eq}, f_{short}(t_m = 25 ms) and f_{short}(t_m = 400 ms) using the Friedman test. * $p < 0.05$, **** $p < 0.0001$. In (**D**), open blue circles represent MSME and REXI data, and dashed red curves are the results of model fitting. **E** The f_{short}-t_m curve from a representative rat. bi-exp. fit, bi-exponential fitting; mono-exp. fit, mono-exponential fitting

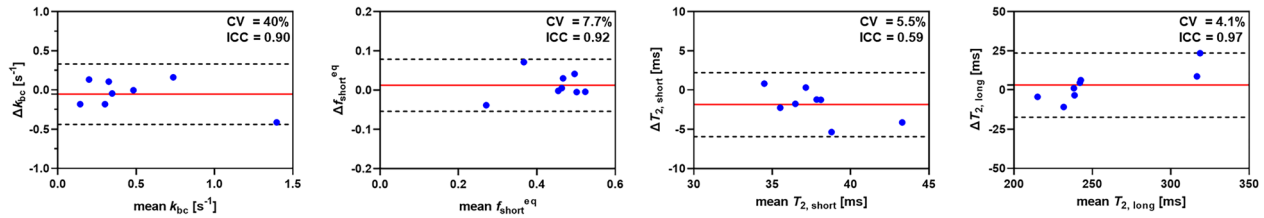

Fig. 4 Scan-rescan reproducibility of k_{bc}, f_{short}^{eq}, $T_{2, long}$, and $T_{2, short}$ depicted via BA plots. The horizontal axis represents the average of two measurements, whereas the vertical axis represents the difference between the two measurements. Solid line and dashed lines in BA plots denote mean difference and mean difference ± 1.96 * standard deviation, respectively

ms (control, $p = 0.0728$). These quantitative results clearly demonstrate the sensitivity and specificity of REXI in measurement of the CP steady-state water efflux rate (k_{bc}).

Discussion

The CP is essential for maintaining CSF homeostasis in the brain. It acts as a primary CSF secretion site and neuroprotective barrier, preventing harmful compounds from accumulating in the CSF and brain tissue. Despite the critical importance of the CP, studies of BCSFB

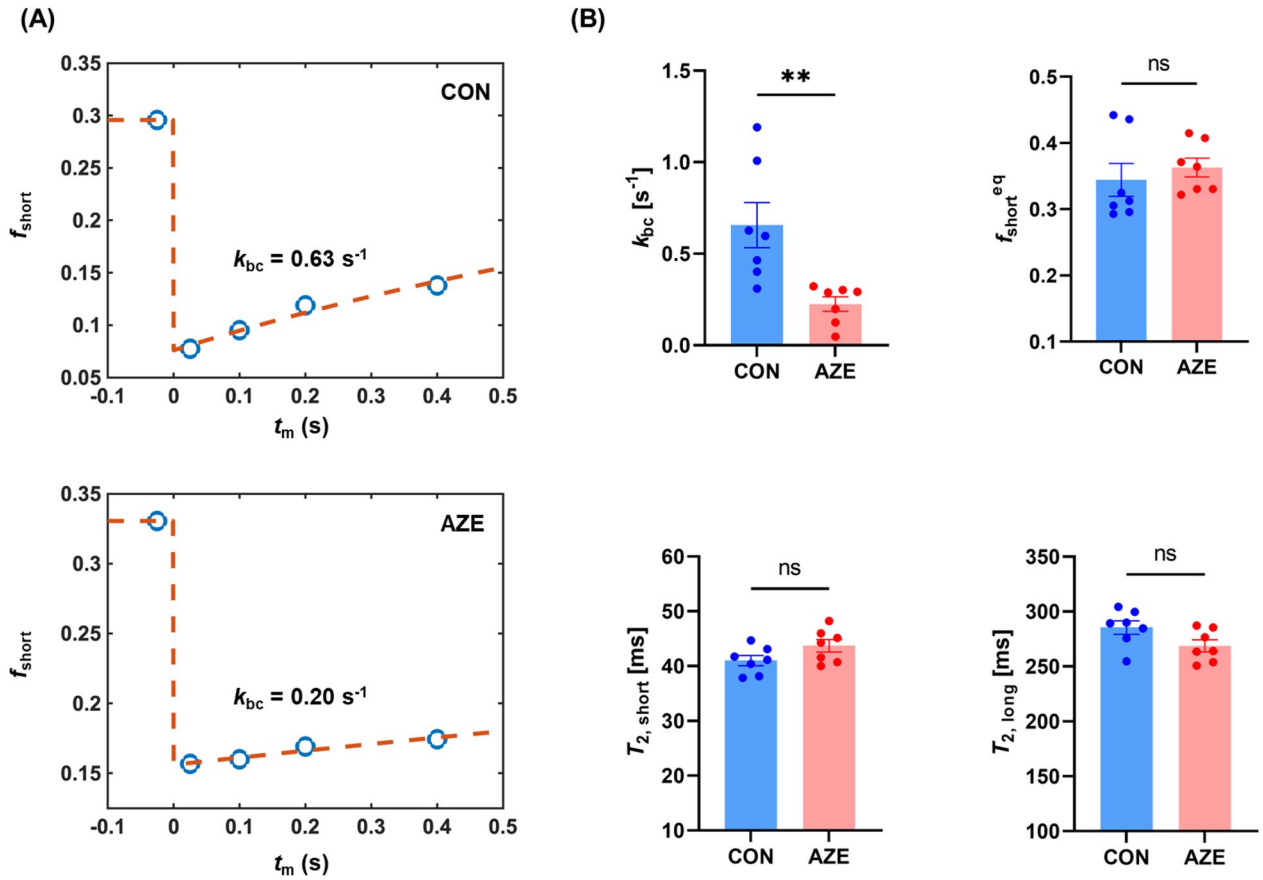

Fig. 5 REXI detection of pharmacologically induced downregulation of CSF secretion via k_{bc} alteration in rats**. A** The f_{short}-t_m curves of representative rats in the treatment and control groups. **B** Statistical comparison of k_{bc}, f_{short}^{eq}, $T_{2, short}$, and $T_{2, long}$ in the rat CP between treatment and control groups. AZE: treatment group with i.v. delivery of acetazolamide, CON: control group with i.v. delivery of vehicle. Mann–Whitney tests. ** $p < 0.01$

function have been limited, primarily due to the lack of a practical, non-invasive measurement technique [12]. In this study, we introduced a non-invasive MRI method, REXI, to assess BCSFB function by measuring the trans-BCSFB water exchange rate in the CP. We demonstrated the ability of REXI to measure exchange processes using a well-established two-pool system: urea-water phantoms with varying pH. In the rat CP, the MSME signal exhibited a clear bi-exponential decay with distinct T_2 values for CP tissue and CSF water. REXI successfully suppressed CP tissue in the filter block, and the expected recovery of the CP tissue component was observed and accurately described by the 2SXM. Further scan-rescan experiments demonstrated the high reproducibility of REXI in measuring the steady-state water efflux rate from CP to CSF. Finally, REXI exhibited high sensitivity to acetazolamide-induced CP dysfunction, revealing a 66% decrease in k_{bc}.

REXI is a specialized version of relaxation exchange spectroscopy (REXSY), a technique widely used in porous media and chemistry to study proton or other molecular exchange in systems with multi-component T_2s [23, 33, 34]. REXI differs from REXSY by offering imaging capabilities and a faster acquisition protocol. This shortened acquisition time is achieved by reducing the three-dimensional data acquisition of REXSY to two dimensions. Specifically, the first multi-echo block in the REXSY experiment is replaced with a fixed T_2-filter block optimized to suppress signals from molecules with shorter T_2 values. A similar strategy has been applied in diffusion exchange spectroscopy (DEXSY) through the development of a clinical MRI version termed filter exchange imaging (FEXI) [29], which fixes the first diffusion weighting to shorten acquisition time. FEXI is now widely used in studies of cell membrane in tumors [30, 35] and also blood–brain barrier [36, 37]. REXI utilizes the difference in T_2s between two components (e.g., CP tissue and CSF), while FEXI exploits the difference in apparent diffusivities between two components (e.g., tissue and blood). The difference between the diffusivities

of CSF ($\sim 3.2\times10^{-9}$ m^2/s) and tissue (e.g., gray matter, $\sim 0.8\times10^{-9}$ m^2/s) [38] is only around fourfold. The blood flow inside the CP could also induce pseudo diffusivity [39], making the apparent diffusivity difference between CSF and CP tissue even smaller. But the difference between T_2 of CSF ($\sim$2000 ms at 3 T) [40] and T_2 of tissue (e.g., gray matter, $\sim$80 ms at 3 T) [41] is much larger, around 25-fold. Thus, REXI can easily filter out the signal of CP tissue without altering the signal of CSF too much in the filter block, whereas it would be much more challenging to use FEXI to achieve this goal. Recently, other non-invasive methods based on the ASL MRI [16, 18, 20, 42] have been developed to measure the water efflux rate from CP to CSF. However, the ASL-based approaches usually require a long acquisition time and are limited by low SNR (signal-to-noise ratio) or low spatial resolution due to the acquisition of both the control and arterial label images and the subtraction of the two images. For example, for small-animal CP function detection, the acquisition time of ASL-based method in [16] is around 48 min and that in [42] is around 45 min, but the acquisition time of our REXI is only $\sim$21 min. Besides, the spatial resolution of our REXI is 0.27 mm$\times$0.36 mm, but the spatial resolution of ASL-based method is only 0.625 mm$\times$0.625 mm in [16] and 1.0 mm$\times$1.0 mm in [42]. These advantages could potentially make REXI a more favorable technique for clinical transfer in the future.

The urea-water phantom is a well-defined two-pool exchange system, in which the exchange rate between water and urea amino protons can be adjusted by varying the pH [25]. In the present study, the proton exchange rate constants detected by REXI were consistent with those reported in previous studies using REXSY [25]. Importantly, REXI also detected an increase in the exchange rate as the pH decreased from 7.0 to 6.7, which aligns with the mechanism of protolysis in standard amides (i.e., proton exchange in urea solutions is acid-catalyzed) [43, 44]. In addition to the exchange rate, the T_2 values of both components decreased with decreasing pH, which matched previous findings of reduced T_2 in urea solutions [45]. This decrease can be further explained by chemical exchange theory [46], which indicates that increased exchange shortens T_2. Taken together, these results demonstrate that REXI can sensitively detect exchange processes within a reasonable scan time.

In the CP, the MSME signal exhibited a clear bi-exponential decay, with a short T_2 of approximately 40 ms and a long T_2 of approximately 270 ms, consistent with reported T_2 values for CP tissue and CSF in rats at 9.4T [20]. The REXI filter block effectively suppressed the blood signal, reducing f_{short} from 0.40 $\pm$ 0.08 to 0.20 $\pm$ 0.06. This reduction was expected based on the T_2 difference between blood and CSF, and it significantly recovered (to 0.25 $\pm$ 0.06) after a mixing time of 400 ms. The changes in f_{short} according to variations in t_m were clearly described by the 2SXM, demonstrating the ability of REXI to capture the water exchange rate between blood and CSF based on differences in T_2 across the two compartments. Further scan-rescan experiments demonstrated the excellent reproducibility of REXI in terms of measuring k_{bc} within the CP (ICC = 0.90), as well as measurement of the blood fraction (f_{short}) and the T_2 values of the two components. The high CV of k_{bc} (40%) may be due to individual physiological differences, as reported by Eisma et al. in their study of CSF flow rates [47]. Another possible source of this high CV could be the relatively short t_m used in the current protocol.

Acetazolamide has been shown to reduce CSF secretion in humans [48, 49] and animal models [50–52], including rats [14, 53]. Acetazolamide is a non-specific carbonic anhydrase inhibitor, effective across various delivery modes (i.v., intracerebroventricular, and intraperitoneal) due to its membrane permeability; thus, it affects both intra- and extracellular carbonic anhydrases [2, 27]. Among the various ion transporters and channels expressed on the CP epithelium, the contribution of HCO_3^- transporters to CSF secretion is well-established [2]. These transporters include the Na^+-driven chloride bicarbonate exchanger (NCBE), Na^+-driven bicarbonate cotransporter e2 (NBCe2), Na^+-driven bicarbonate cotransporter n1 (NBCn1), and anion exchanger 2 (AE2; a Cl^-/HCO_3^- exchanger) [54, 55]. The activities of these transporters rely on the presence of their substrate, HCO_3^-. Acetazolamide inhibits several carbonic anhydrases localized in the CP, hindering the conversion of CO_2 to H_2CO_3 and reducing HCO_3^- generation; this process impacts bicarbonate transporter-mediated CSF production [27]. In the present study, REXI also revealed a 66% reduction in k_{bc}, comparable to the 40% reduction in acetazolamide-mediated CSF secretion observed by fluorescent imaging [27]; this result demonstrated REXI's sensitivity to CP dysfunction.

In this study, we chose to use and report the steady-state water efflux rate from CP tissue (essentially blood) to CSF, k_{bc}, rather than the steady-state water exchange rate from CSF to CP (k_{cb}) or the overall exchange rate between CP and CSF k ($=k_{bc}+k_{cb}$). The k_{bc} is a physical parameter and an independent biomarker that describes the barrier permeability and is not sensitive to the partial volume effect as

$$k_{bc} = P < \frac{A_{CP}}{V_{CP}} >$$

where P is the water permeability coefficient of CP-CSF barrier (the choroid plexus epithelial cell), $< \frac{A_{CP}}{V_{CP}} >$ is the surface to volume ratio of CP tissue. Considering the fact

that the CP is a network of capillaries lined by epithelial cells and assuming the capillaries as cylinders with radius r, $< \frac{A_{CP}}{V_{CP}} >$ of these capillaries would be $2/r$ and a constant if the size of capillary doesn't change. This makes k_{bc} insensitive to the CSF volume fraction in each voxel and a direct biomarker of the water permeability coefficient of the CP-CSF barrier. On the other hand, the steady-state water exchange rate from CSF to CP (k_{cb}) is,

$$k_{cb} = P < \frac{A_{CP}}{V_{CSF}} >$$

where V_{CSF} is the CSF volume in each voxel. As REXI still has a very low spatial resolution, V_{CSF} can vary across voxels and experiments due to the partial volume effect, which would induce k_{cb} to be strongly biased by the V_{CSF} in each voxel. The overall exchange rate between CP and CSF k ($=k_{bc}+k_{cb}$) would also depend on V_{CSF} and thus is not an independent biomarker of barrier permeability to water. Similar choices have been made to describe the cell membrane permeability to water and BBB permeability to water, which are the steady-state intracellular water efflux rate [56] and steady-state intravascular water efflux rate [36].

REXI measures the water exchange rates between the CP and CSF, rather than the net water secretion rate from CP to CSF, and the exchange is expected to be much faster than the net water secretion. Considering the CSF production rate in rats (approximately 1.40 μL/min [14]) and the volume of CP tissue (1.21 mm^3), the net water secretion flux rate from CP to CSF is approximately 0.02 s^{-1}. Given the mean $k_{bc}=0.49$ s^{-1} in the rat CP of the scan-rescan experiment measured in this study, the unidirectional water efflux greatly exceeds the net CSF secretion flux [57], supporting the steady-state assumption in the 2SXM. Therefore, only one in 200 water molecules cycled through the CP tissue (e.g., epithelial cells) is transported into the CSF without immediate return. However, the water exchange between CP and CSF and the net water secretion from CP to CSF are two closely linked processes, making k_{bc} an indirect but sensitive biomarker of CSF secretion. This is because both processes are facilitated by the ion transporters and the Na^+-K^+-ATPase pump located on the membrane of CP epithelium [17]. CSF (including water) production is an active metabolic process as CSF contains a higher concentration of Na^+ and a lower concentration of K^+ than would be expected from an ultrafiltrate from plasma [54]. The driving force of these ion transporters would eventually be tracked back to the Na^+-K^+-ATPase pump, which is largely expressed in the apical membrane of CP epithelium and the suppression of whose activity with ouabain could largely reduce CSF secretion rate [51, 58]. Water exchange across cell membrane can also be facilitated by ion transports as many of them are also water cotransporters [59], and driven by the Na^+-K^+-ATPase activity [31, 60]. For example, on the membrane of CP epithelium, $Na^+/K^+/2Cl^-$ cotransporter 1 (NKCC1) is a well-established water cotransporter, in which there are 590 water molecules transported per turn over [61]. At the same time, NKCC1 also plays a key role in CSF secretion [62–64]. Although the studies of the water cotransporting capacity of HCO_3^- transporters are still limited, evidence has shown that administration of acetazolamide could also slow down the activity of the Na^+-K^+-ATPase pump [65], which could then induce slower trans-membrane water exchange observed in this study. More studies are still highly needed to clarify the major molecular pathways governing the trans-membrane water exchange and water secretion in CP, though this remains technically challenging.

Several limitations and future directions of this study should be clarified. First, the T_1s of the CP tissue and CSF are assumed to be same in the current analysis model of REXI. Indeed, it is difficult to decouple the T_1 relaxation and exchange when the T_1s of CP tissue and CSF are different [66]. The influence on exchange estimation is largely dependent on the ratio between exchange rate k ($=k_{bc}+k_{cb}$) and R_1 difference (ΔR_1), i.e., more bias in exchange estimation is expected when $\Delta R_1/k$ is larger [29]. Fortunately, the R_1s of CP tissue (using cortex value) and CSF at 9.4 T are very close (0.53 s^{-1} and 0.41 s^{-1}, respectively, [67]), resulting in a very small ΔR_1 ($=0.12$ s^{-1}) and ΔR_1/k ($=14\%$, taking $k_{bc}=0.49$ s^{-1} and CP volume fraction ~ 0.44, the average results of all rats in the scan-rescan experiment of this study). With such a small ΔR_1, we would expect the effect of R_1 difference on the exchange estimation to be limited. In addition, considering the R_1s of each site would not change dramatically even in pathological conditions, a possible solution in the future is to fix the R_1s of each site as constant values to remove the potential bias in exchange estimation. Second, other REXI acquisition parameters, such as the selection of single or multiple TE_f values and the combination of several t_m values, could be optimized to improve the precision of exchange estimation. A recent paper proposed an optimization pipeline specifically for this type of NMR/MRI experiments [35], which can be implemented for REXI optimization in the future. Third, we used a relatively high concentration of 2.5% isoflurane to minimize the head motion of rats. Compared to the awake state, the CSF production rate is increased in mice under isoflurane anesthesia [15], which might lead to an overestimation in our measurements. Additionally, because of its novelty, future studies should compare REXI with other methods (e.g., invasive methods)

to further validate its feasibility in animal models and humans. We anticipate that REXI will be utilized to elucidate the molecular mechanisms of water transport in the BCSFB and the regulation of the CP by circadian rhythm. It would also be useful to incorporate REXI into explorations of age-dependence regarding BCSFB water permeability and CP dysfunction in neurological disorders, such as traumatic brain injury and Alzheimer's disease.

Conclusions

REXI is a novel method for measuring trans-barrier water exchange between the CP and CSF, based on the large T_2 difference between these two components. This proof-of-concept study established this technique for non-invasive and quantitative assessments of BCSFB function. Considering the multifaceted role of the BCSFB in maintaining brain homeostasis, this method exhibits great potential for enhancing analyses and clinical management of brain disorders.

Abbreviations

AIC	Akaike Information Criterion
ASL	Arterial spin labeling
BA	Bland–Altman
BCSFB	Blood-cerebrospinal fluid barrier
CP	Choroid plexus
CSF	Cerebrospinal fluid
CV	Coefficient of variation
DEXSY	Diffusion exchange spectroscopy
FEXI	Filter exchange imaging
FOV	Field of view
ICC	Intraclass correlation coefficient
i.v.	Intravenous
ME	Multi-echo
MRI	Magnetic resonance imaging
MSME	Multi-slice Multi-echo
NA	Number of averages
NE	Number of echoes
NMR	Nuclear magnetic resonance
RARE	Rapid acquisition with relaxation enhancement
REXI	Relaxation-exchange magnetic resonance imaging
REXSY	Relaxation exchange spectroscopy
ROI	Region of interest
SNR	Signal-to-noise ratio
TE	Echo time
TR	Repetition time
WKY	Wistar Kyoto
2SXM	Two-site exchange model

Acknowledgements
Not applicable

Author contributions
The contribution of the authors was as follows: Conceptualization—RB, RX, XW, YY, YH; Methodology—XW, RB, YH, BZ; Experimental design—XW, QH, YY, WL, RB; Data acquisition and analysis—XW, QH, YY, ST; Interpretation—XW, QH, YY, YH, RB; Drafting of manuscript—XW, RB, RX. All authors read and approved the final manuscript.

Funding
The study was supported by the National Key Research and Development Program of China (grants 2022ZD0206000, 2022ZD0211901), the National Natural Science Foundation of China (grants 82222032, 82111530201), the Ministry of Science and Technology of China (grant 2019YFA0707103), and the Key R&D Program of Zhejiang Province (2024SSYS0019).

Availability of data and materials
The datasets used and/or analyzed during the current study are available from the corresponding author on reasonable request.

Declarations

Ethics approval and consent to participate
Animal experiments were approved by the Animal Experimentation Committee of Zhejiang University.

Consent for publication
Not applicable.

Competing interests
The authors declare no competing interests.

Author details
[1]State Key Laboratory of Brain and Cognitive Science, Beijing MRI Center for Brain Research, Institute of Biophysics, Chinese Academy of Sciences, Beijing, China. [2]University of Chinese Academy of Sciences, Beijing, China. [3]School of Brain Science and Brain Medicine, Zhejiang University, Hangzhou, China. [4]Interdisciplinary Institute of Neuroscience and Technology and Liangzhu Laboratory, Zhejiang University School of Medicine, Hangzhou, China. [5]Department of Chemistry, Zhejiang University, Hangzhou, China. [6]Key Laboratory of Biomedical Engineering of Education Ministry, College of Biomedical Engineering and Instrument Science, Zhejiang University, Hangzhou, China. [7]Key Laboratory of Novel Targets and Drug Study for Neural Repair of Zhejiang Province, School of Medicine, Hangzhou City University, Hangzhou, China. [8]MR Collaboration, Siemens Healthcare, Shanghai, China.

Received: 30 July 2024 Accepted: 23 October 2024
Published online: 26 November 2024

References

1. Bitanihirwe BKY, Lizano P, Woo TUW. Deconstructing the functional neuroanatomy of the choroid plexus: an ontogenetic perspective for studying neurodevelopmental and neuropsychiatric disorders. Mol Psychiatry. 2022;27:3573–82.
2. MacAulay N, Keep RF, Zeuthen T. Cerebrospinal fluid production by the choroid plexus: a century of barrier research revisited. Fluids Barriers CNS. 2022;19:26.
3. Saunders NR, Dziegielewska KM, Fame RM, Lehtinen MK, Liddelow SA. The choroid plexus: a missing link in our understanding of brain development and function. Physiol Rev. 2023;103:919–56.
4. Lun MP, Monuki ES, Lehtinen MK. Development and functions of the choroid plexus–cerebrospinal fluid system. Nat Rev Neurosci. 2015;16:445–57.
5. Bothwell SW, Janigro D, Patabendige A. Cerebrospinal fluid dynamics and intracranial pressure elevation in neurological diseases. Fluids Barriers CNS. 2019;16:9.
6. Solár P, Zamani A, Kubíčková L, Dubový P, Joukal M. Choroid plexus and the blood–cerebrospinal fluid barrier in disease. Fluids Barriers CNS. 2020;17:35.
7. Cousins O, Hodges A, Schubert J, Veronese M, Turkheimer F, Miyan J, et al. The blood–CSF–brain route of neurological disease: the indirect pathway into the brain. Neuropathology Appl Neurobio. 2022;48: e12789.
8. Municio C, Carrero L, Antequera D, Carro E. Choroid plexus aquaporins in CSF homeostasis and the glymphatic system: their relevance for Alzheimer's disease. IJMS. 2023;24:878.
9. Quintela T, Furtado A, Duarte AC, Gonçalves I, Myung J, Santos CRA. The role of circadian rhythm in choroid plexus functions. Prog Neurobiol. 2021;205: 102129.
10. Christensen J, Li C, Mychasiuk R. Choroid plexus function in neurological homeostasis and disorders: the awakening of the circadian clocks and orexins. J Cereb Blood Flow Metab. 2022;42:1163–75.

11. Pappenheimer JR, Heisey SR, Jordan EF, de Downer JC. Perfusion of the cerebral ventricular system in unanesthetized goats. Am J Physiol Legacy Content. 1962;203:763–74.
12. Liu G, Ladrón-de-Guevara A, Izhiman Y, Nedergaard M, Du T. Measurements of cerebrospinal fluid production: a review of the limitations and advantages of current methodologies. Fluids Barriers CNS. 2022;19:101.
13. Flexner LB, Winters H. The rate of formation of cerebrospinal fluid in etherized cats. Am J Physiol Legacy Content. 1932;101:697–710.
14. Karimy JK, Kahle KT, Kurland DB, Yu E, Gerzanich V, Simard JM. A novel method to study cerebrospinal fluid dynamics in rats. J Neurosci Methods. 2015;241:78–84.
15. Liu G, Mestre H, Sweeney AM, Sun Q, Weikop P, Du T, et al. Direct measurement of cerebrospinal fluid production in mice. Cell Rep. 2020;33: 108524.
16. Evans PG, Sokolska M, Alves A, Harrison IF, Ohene Y, Nahavandi P, et al. Non-invasive mri of blood-cerebrospinal fluid barrier function. Nat Commun. 2020;11:2081.
17. Anderson VC, Tagge IJ, Doud A, Li X, Springer CS, Quinn JF, et al. DCE-MRI of brain fluid barriers: in vivo water cycling at the human choroid plexus. Tissue Barriers. 2022;10:1963143.
18. Zhao L, Taso M, Dai W, Press DZ, Alsop DC. Non-invasive measurement of choroid plexus apparent blood flow with arterial spin labeling. Fluids Barriers CNS. 2020;17:58.
19. Wells JA, Siow B, Lythgoe MF, Thomas DL. Measuring biexponential transverse relaxation of the asl signal at 9.4 t to estimate arterial oxygen saturation and the time of exchange of labeled blood water into cortical brain tissue. J Cereb Blood Flow Metab. 2013;33:215–24.
20. Lee H, Ozturk B, Stringer MS, Koundal S, MacIntosh BJ, Rothman D, et al. Choroid plexus tissue perfusion and blood to CSF barrier function in rats measured with continuous arterial spin labeling. Neuroimage. 2022;261: 119512.
21. Vold RL, Daniel ES, Chan SO. Magnetic resonance measurements of proton exchange in aqueous urea. J Am Chem Soc. 1970;92:6771–6.
22. Lee JH, Labadie C, Springer CS, Harbison GS. Two-dimensional inverse Laplace transform NMR: altered relaxation times allow detection of exchange correlation. J Am Chem Soc. 1993;115:7761–4.
23. Bai R, Benjamini D, Cheng J, Basser PJ. Fast, accurate 2D-MR relaxation exchange spectroscopy (REXSY): Beyond compressed sensing. J Chem Phys. 2016;145: 154202.
24. Stabinska J, Neudecker P, Ljimani A, Wittsack H, Lanzman RS, Müller-Lutz A. Proton exchange in aqueous urea solutions measured by water-exchange (WEX) NMR spectroscopy and chemical exchange saturation transfer (CEST) imaging in vitro. Magn Reson Med. 2019;82:935–47.
25. Dortch RD, Horch RA, Does MD. Development, simulation, and validation of NMR relaxation-based exchange measurements. J Chem Phys. 2009;131: 164502.
26. Ames A, Higashi K, Nesbett FB. Effects of Pco2 acetazolamide and ouabain on volume and composition of choroid-plexus fluid. J Physiol. 1965;181:516–24.
27. Barbuskaite D, Oernbo EK, Wardman JH, Toft-Bertelsen TL, Conti E, Andreassen SN, et al. Acetazolamide modulates intracranial pressure directly by its action on the cerebrospinal fluid secretion apparatus. Fluids Barriers CNS. 2022;19:53.
28. Åslund I, Nowacka A, Nilsson M, Topgaard D. Filter-exchange PGSE NMR determination of cell membrane permeability. J Magn Reson. 2009;200:291–5.
29. Lasič S, Nilsson M, Lätt J, Ståhlberg F, Topgaard D. Apparent exchange rate mapping with diffusion MRI. Magn Reson Med. 2011;66:356–65.
30. Nilsson M, Lätt J, Van Westen D, Brockstedt S, Lasič S, Ståhlberg F, et al. Noninvasive mapping of water diffusional exchange in the human brain using filter-exchange imaging. Magn Reson Med. 2013;69:1572–80.
31. Bai R, Springer CS, Plenz D, Basser PJ. Fast, Na^+/K^+ pump driven, steady-state transcytolemmal water exchange in neuronal tissue: A study of rat brain cortical cultures. Magn Reson Med. 2018;79:3207–17.
32. Akaike H. A new look at the statistical model identification. IEEE Trans Autom Control. 1974;19:716–23.
33. Washburn KE, Callaghan PT. Tracking pore to pore exchange using relaxation exchange spectroscopy. Phys Rev Lett. 2006;97: 175502.
34. Ullah MS, Mankinen O, Zhivonitko VV, Telkki V-V. Ultrafast transverse relaxation exchange NMR spectroscopy. Phys Chem Chem Phys. 2022;24:22109–14.
35. Lampinen B, Szczepankiewicz F, van Westen D, Englund E, Sundgren PC, Lätt J, et al. Optimal experimental design for filter exchange imaging: apparent exchange rate measurements in the healthy brain and in intracranial tumors. Magn Res Med. 2017;77:1104–14.
36. Bai R, Li Z, Sun C, Hsu YC, Liang H, Basser P. Feasibility of filter-exchange imaging (FEXI) in measuring different exchange processes in human brain. Neuroimage. 2020;219: 117039.
37. Zhang Y, Wang Y, Li Z, Wang Z, Cheng J, Bai X, et al. Vascular-water-exchange MRI (VEXI) enables the detection of subtle AXR alterations in Alzheimer's disease without MRI contrast agent, which may relate to BBB integrity. Neuroimage. 2023;270: 119951.
38. Pierpaoli C, Jezzard P, Basser PJ, Barnett A, Di Chiro G. Diffusion tensor MR imaging of the human brain. Radiology. 1996;201:637–48.
39. Le Bihan D. What can we see with IVIM MRI? Neuroimage. 2019;187:56–67.
40. Spijkerman JM, Petersen ET, Hendrikse J, Luijten P, Zwanenburg JJM. T 2 mapping of cerebrospinal fluid: 3 T versus 7 T. Magn Reson Mater Phy. 2018;31:415–24.
41. Uludağ K, Müller-Bierl B, Uğurbil K. An integrative model for neuronal activity-induced signal changes for gradient and spin echo functional imaging. Neuroimage. 2009;48:150–65.
42. Perera C, Tolomeo D, Baker RR, Ohene Y, Korsak A, Lythgoe MF, et al. Investigating changes in blood-cerebrospinal fluid barrier function in a rat model of chronic hypertension using non-invasive magnetic resonance imaging. Front Mol Neurosci. 2022;15: 964632.
43. Berger A, Loewenstein A, Meiboom S. Nuclear magnetic resonance study of the protolysis and ionization of N-Methylacetamide [1]. J Am Chem Soc. 1959;81:62–7.
44. Klotz IM, Hunston DL. Proton exchange in aqueous urea solutions. J Phys Chem. 1971;75:2123–7.
45. Connor S, Nicholson JK, Everett JR. Chemical-exchange and paramagnetic T2 relaxation agents for water suppression in spin-echo proton nuclear magnetic resonance spectroscopy of biological fluids. Anal Chem. 1987;59:2885–91.
46. Brooks RA, Moiny F, Gillis P. On T_2 -shortening by weakly magnetized particles: the chemical exchange model†. Magn Reson Med. 2001;45:1014–20.
47. Eisma JJ, McKnight CD, Hett K, Elenberger J, Song AK, Stark AJ, et al. Choroid plexus perfusion and bulk cerebrospinal fluid flow across the adult lifespan. J Cereb Blood Flow Metab. 2023;43:269–80.
48. Rubin RC, Henderson ES, Ommaya AK, Walker MD, Rall DP. The production of cerebrospinal fluid in man and its modification by acetazolamide. J Neurosurg. 1966;25:430–6.
49. Carrion E. Use of acetazolamide to decrease cerebrospinal fluid production in chronically ventilated patients with ventriculopleural shunts. Arch Dis Child. 2001;84:68–71.
50. Tschirgi RD, Frost RW, Taylor JL. Inhibition of cerebrospinal fluid formation by a carbonic anhydrase inhibitor, 2-acetylamino-1, 3, 4-thiadiazole-5-sulfonamide (Diamox). Exp Biol Med. 1954;87:373–6.
51. Davson H, Segal MB. The effects of some inhibitors and accelerators of sodium transport on the turnover of ^{22} Na in the cerebrospinal fluid and the brain. J Physiol. 1970;209:131–53.
52. Holloway LS, Cassin S. Effect of acetazolamide and ouabain on CSF production rate in the newborn dog. Am J Physiol Legacy Content. 1972;223:503–6.
53. Vogh BP, Godman DR, Maren TH. Effect of AlCl3 and other acids on cerebrospinal fluid production: a correction. J Pharmacol Exp Ther. 1987;243:35.
54. MacAulay N. Molecular mechanisms of brain water transport. Nat Rev Neurosci. 2021;22:326–44.
55. Xiang J, Hua Y, Xi G, Keep RF. Mechanisms of cerebrospinal fluid and brain interstitial fluid production. Neurobiol Dis. 2023;183: 106159.
56. Li Z, Pang Z, Cheng J, Hsu Y-C, Sun Y, Özarslan E, et al. The direction-dependence of apparent water exchange rate in human white matter. Neuroimage. 2021;247: 118831.
57. Hladky SB, Barrand MA. Fluid and ion transfer across the blood–brain and blood–cerebrospinal fluid barriers; a comparative account of mechanisms and roles. Fluids Barriers CNS. 2016;13:19.

58. Welch K. Secretion of cerebrospinal fluid by choroid plexus of the rabbit. Am J Physiol Legacy Content. 1963;205:617–24.
59. Zeuthen T. Molecular water pumps. Reviews of Physiology Biochemistry and Pharmacology. Berlin, Heidelberg: Springer Berlin Heidelberg; 2000, p. 97–151.
60. Springer CS. Using 1H2O MR to measure and map sodium pump activity in vivo. J Magn Reson. 2018;291:110–26.
61. Zeuthen T. Water-transporting proteins. J Membrane Biol. 2010;234:57–73.
62. Steffensen AB, Oernbo EK, Stoica A, Gerkau NJ, Barbuskaite D, Tritsaris K, et al. Cotransporter-mediated water transport underlying cerebrospinal fluid formation. Nat Commun. 2018;9:2167.
63. Oernbo EK, Steffensen AB, Razzaghi Khamesi P, Toft-Bertelsen TL, Barbuskaite D, Vilhardt F, et al. Membrane transporters control cerebrospinal fluid formation independently of conventional osmosis to modulate intracranial pressure. Fluids Barriers CNS. 2022;19:65.
64. Rasmussen MK, Mestre H, Nedergaard M. Fluid transport in the brain. Physiol Rev. 2022;102:1025–151.
65. Uldall M, Botfield H, Jansen-Olesen I, Sinclair A, Jensen R. Acetazolamide lowers intracranial pressure and modulates the cerebrospinal fluid secretion pathway in healthy rats. Neurosci Lett. 2017;645:33–9.
66. Van Landeghem M, Haber A, D'espinose De Lacaillerie J, Blümich B. Analysis of multisite 2D relaxation exchange NMR. Concepts Magn Reson. 2010;36A:153–69.
67. Van De Ven RCG, Hogers B, Van Den Maagdenberg AMJM, De Groot HJM, Ferrari MD, Frants RR, et al. T_1 relaxation in in vivo mouse brain at ultra-high field. Magn Reson Med. 2007;58:390–5.

Publisher's Note